CPC(HEP & NP), 2009, 33(11): 949—953 Chinese Physics C Vol. 33, No. 11, Nov., 2009

High resolution X-ray diffraction investigation of epitaxially grown $SrTiO_3$ thin films by laser-MBE*

ZHAI Zhang-Yin(翟章印)[1,2] WU Xiao-Shan(吴小山)[1;1)] JIA Quan-Jie(贾全杰)[3]

1 (Lab of Solid State Microstructures and Department of Physics, Nanjing University, Nanjing 210093, China)
2 (Jiangsu Key Laboratory for Chemistry of Low-Dimensional Materials and Department of Physics, Huaiyin Normal University, Huaian 223300, China)
3 (BSRF, Institute of High Energy Physics, CAS, Beijing 100049, China)

Abstract $SrTiO_3$ thin films are epitaxially grown on $DyScO_3$, $LaAlO_3$ substrates with/without buffer layers of $DyScO_3$ and $SrRuO_3$ using laser-MBE. X-ray diffraction methods, such as high resolution X-ray diffraction, grazing incident X-ray diffraction, and reciprocal space mapping are used to investigate the lattice structure, dislocation density, in-plane lattice strain distribution along film thickness. From the measurement results, the effects of substrate on film lattice quality and microstructure are discussed.

Key words laser-MBE, grazing incident X-ray diffraction, reciprocal space mapping

PACS 68.37.Og

1 Introduction

$SrTiO_3$ (STO) is an incipient ferroelectric or quantum paraelectric material, which remains paraelectric down to 0 K while a second order structural phase transition happens at the temperature of 105 K for the bulk STO crystals. The unit cell decreases from cubic (space group Pm3m) to tetragonal (space group I4/mcm)[1]. This phase transition results from the rotation of TiO_2 plane in TiO_6 octahedron along longer c-axes, in which two proximate octahedrons have opposite rotation directions. Although the ferroelectric properties were only reported through cation substitution[2, 3] and oxygen isotope exchange $ST^{18}O$[4], recent theories and experiments validate the existence of ferroeletricity in STO thin films under strain[5—7].

On the other hand, Feizhou He[8, 9] has systematically studied the structural phase transition of STO thin films under strain, and found that the phase transition temperature was connected with strain. Strain also plays a crucial role in affecting their physical properties on other materials, such as ferroelectric[10, 11] and superconductor[12, 13].

As we know, strain is mainly induced by the mismatch of lattice constant and the difference of thermal expansion coefficient between films and substrates. In this paper, we investigate the strain distribution, dislocation density in STO thin films deposited on $DyScO_3$ (DSO), $LaAlO_3$ (LAO) substrates, and $SrRuO_3$ (SRO) and DSO buffered LAO substrates.

2 Experiments

A single crystal STO and high pure ceramic DSO and SRO targets were used to grow STO film and the buffer layers. (110)-oriented DSO and (100)-oriented LAO single crystals were used as the substrates, which were cleaned carefully before they were put into the chamber. The STO films were deposited in an oxygen pressure of 1.4×10^{-1} mbar at the temperature of 800 ℃ while the buffer layers were deposited at 600 ℃. The deposited films were cooled down to room temperature in an oxygen atmosphere of 600 mbar after 30 minutes. The buffer layers were 20 nm thick and the films were 80, 100 and 150 nm thick from the measurement of a Dektax[3]ST surface profile. X-ray diffraction (XRD, Cu Kα radiation) analysis was made using $\theta/2\theta$ scan on Rigaku Dmax-rB, Bruker advanced D8 X-ray difractometers.

Received 17 December 2008, Revised 2 April 2009

* Supported by National Natural Science Foundation of China (10774065) and Science Foundation for Excellent Youth Scholars of Huaiyin Normal University (08QNZCK 005)

1) E-mail: xswu@nju.edu.cn

©2009 Chinese Physical Society and the Institute of High Energy Physics of the Chinese Academy of Sciences and the Institute of Modern Physics of the Chinese Academy of Sciences and IOP Publishing Ltd

To determine the dislocation density, high resolution XRD, grazing incident X-ray diffraction (surface X-ray diffraction) and reciprocal space mapping (RSM) were carried out on Siemens D5000HR and the X-ray Diffuse Scattering Station on the 4W1C Beam-line of the Beijing Synchrotron Radiation Facility (BSRF).

3 Results and discussions

STO has a cubic structure, with the lattice parameter of $a = 3.905$Å, while DSO has an orthorhombic structure, with the lattice parameter of $a = 5.440$Å, $b = 5.713$Å, $c = 7.887$Å. But the (110) DSO has a near square surface with an in-plane lattice parameter of $a = 3.944$Å (half of the diagonal), resulting in a tensile lattice mismatch of +1.0% with (100) STO at room temperature. Half of c axis lattice parameter is about 3.943Å, and so the DSO substrate can be taken as a pseudocubic structure. SRO also has an orthorhombic structure, with the lattice parameter of $a = 5.563$Å, $b = 5.530$Å, $c = 7.844$Å. We can regard it as pseudocubic structure too, with lattice parameter of $a = 3.920$Å, which has a tensile mismatch of only +0.38% with STO while LAO has a pseudocubic structure, with the lattice parameter of $a = 3.790$Å, resulting in a compressive lattice mismatch of −3.0% with STO.

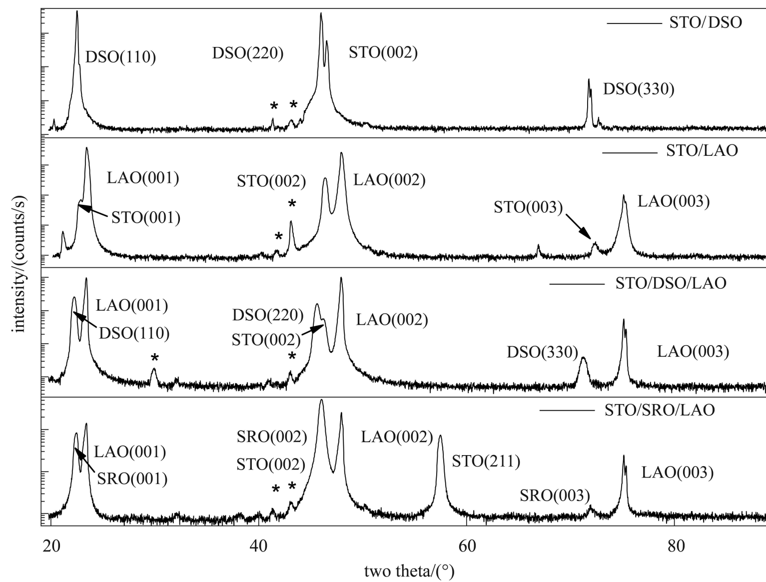

Fig. 1. Room temperature XRD $\theta/2\theta$ scan for STO films with different substrates.

Figure 1 shows a typical room temperature XRD $\theta/2\theta$ scan curve of the STO thin films grown on all kinds of substrates as shown in Table 1. For STO/DSO, STO/LAO and STO/DSO/LAO films, we can just find (001) reflections. However, except for the (001) reflections, the (211) peak is also observed for the STO/SRO/LAO film. The little peaks marked by "∗" were induced by the sample holder.

To further confirm the epitaxial structure, high resolution X-ray diffraction ϕ scan was also carried out. We find they are all strictly fourfold symmetric. Fig. 2 shows the symmetric and asymmetric rocking curves for all samples. The Full Width at Half Max. (FWHM) of (002) symmetric and (103) asymmetric rocking curve is shown in Table 1. We can find that the STO/DSO and STO/LAO films have a much better lattice quality than the STO/SRO/LAO and STO/DSO/LAO films. That's because the SRO and DSO buffer layers were deposited at relatively low temperature, and induced the appearance of abundant defect in the layer, and then caused the STO thin films to grow with relatively poor quality.

High resolution X-ray diffraction symmetric and asymmetric rocking curve can also be used to detect the relaxation induced mismatch dislocation densities (MD). For a given reflection, the measured rocking-curve FWHM $\beta_{\rm m}$ including the intrinsic half width $\beta_{\rm i}$ for the perfect sample is given by[14]:

$$\beta_{\rm m}^2 = \beta_{\rm i}^2 + \beta_{\rm d}^2 + \beta_{\varepsilon}^2 + \beta_{\alpha}^2 + \beta_{\rm L}^2 + \beta_{\rm r}^2 \,. \qquad (1)$$

The intrinsic rocking curve width for the crystal is usually less than several tens of arcseconds and can often be neglected. $\beta_{\rm d}$ is the intrinsic rocking curve width from the diffractometer; β_{ε}, β_{α}, $\beta_{\rm L}$ and $\beta_{\rm r}$ are the rocking curve broadening caused by the strain surrounding dislocations, lattice tilting, particle size

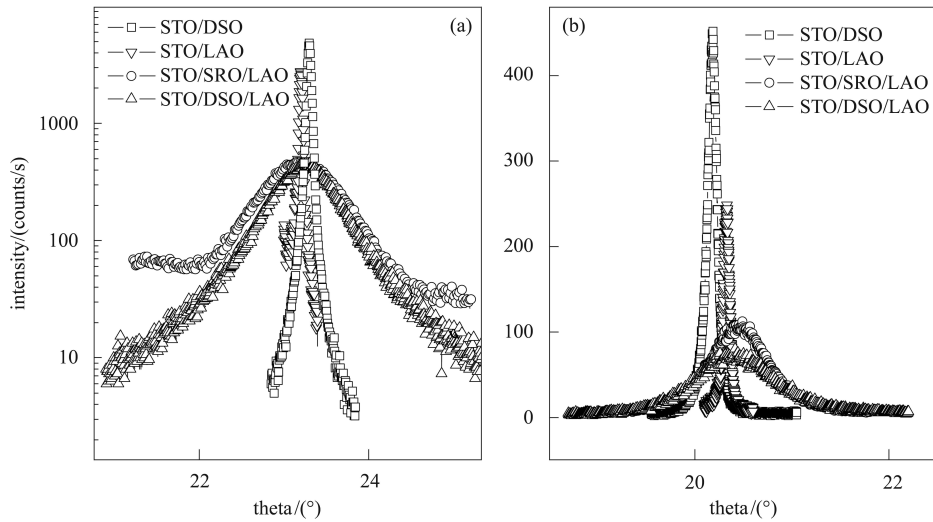

Fig. 2. (002) symmetric (a) and (103) asymmetric (b) rocking curves.

and curvature respectively. The effect of curvature of the sample can be generally neglected owing to the thickness of the substrate compared with that of the layer. Due to the epitaxial relationship between the film and substrate, as have been discussed before, the particle size and lattice tilting broadening can also be neglected here. That's only the first aspect that is taken into account. In such cases:

$$(\Delta\beta)^2 \approx \beta_{\mathrm{m}}^2 - \beta_{\mathrm{i}}^2 - \beta_{\mathrm{d}}^2 \approx \beta_{\varepsilon}^2 \qquad (2)$$

We calculate the dislocation density in STO thin films by using a simplified model[15] $D_{\mathrm{dis}} \approx (\Delta\beta)^2/9b^2$, where, $\Delta\beta$ is the FWHM caused by dislocation, and b is the Burger vector.

Something which needs to mention is that the specific MD geometry in a film will lead to the distortions of only specific crystallographic planes[16]. In general, We consider a (001) film can have either an edge or a screw MD with a [001] line direction. Then the symmetric (001) rocking curves are sensitive only to the screw MD and /or mixed dislocations content in the films and the edge MD will distort only the (hkl) planes with either h or k nonzero. The rocking curves on asymmetric planes, such as (103) plane, will be broadened because these planes are distorted by both the edge and screw MD and /or mixed dislocations.

From the above discussion and the formula, the total MD density can be calculated by using the (103) rocking curve broadening. We find the total dislocation density in buffered films is two orders of magnitude higher than the directly grown films as shown in Table 1. In Fig. 3, the AFM measurement indicates that the directly grown films have root-mean-square (Rms) roughness of 0.19 nm and 0.26 nm, while the two buffered films have Rms roughness of 3.86 nm and 10.77 nm, respectively. This also proves the first two films have a better lattice quality than that of the latter two.

Table 1. Dislacation density and surface roughness for STO films deposited on different substrates.

sample/nm	FWHM/(°)		D_{dis}	Rms
	(002)	(103)	/cm^2	/nm
STO(100)/DSO	0.0443	0.0781	1.35×10^8	0.19
STO(80)/LAO	0.0505	0.1104	2.71×10^8	0.26
STO(100)/DSO/LAO	0.8734	0.7396	1.21×10^{10}	3.86
STO(100)/SRO/LAO	0.9831	0.9460	1.99×10^{10}	10.77

Grazing incidence X-ray diffraction (GIXRD) is applied to determine the distribution of lattice strain along the inner surface normal (i.e., the depth dependence of the lattice strain). GIXRD is a kind of technology sensitive to surface structure of materials. According to the refraction principle, the angle of total reflection can be calculated[17]:

$$\alpha_{\mathrm{c}} = \sqrt{2\delta} = \sqrt{\frac{N_{\mathrm{A}} r_{\mathrm{e}} Z \rho}{A\pi}}\ \lambda\,, \qquad (3)$$

where, N_{A} is the Avogadro Constant, r_{e} is the electronic classic radius, ρ is the density of the material, Z is the atomic number, A is the molecular weight, and λ is the wavelength of X-ray. When the grazing incidence angle is less than the angle of the total reflection ($\alpha_{\mathrm{i}} < \alpha_{\mathrm{c}}$), the penetration depth of X-ray L follows the formula as follows:

$$L = \frac{\lambda}{2\pi\sqrt{2\delta - \sin^2\alpha_{\mathrm{i}}}}\,, \qquad (4)$$

L has a minimal value of 45Å for STO with $\lambda = 1.5406$Å. If the grazing incidence angle is larger than the angle of the total reflection, the penetration depth

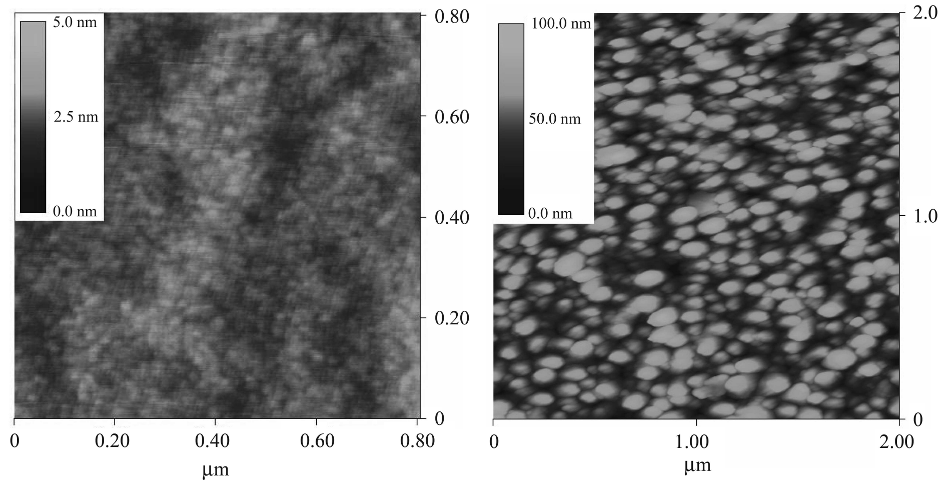

Fig. 3. Surface morphology AFM scan for STO(100 nm)/LAO and STO(100 nm)/ SRO/ LAO films.

of X-ray L is approximately expressed as[18]:

$$L=\frac{1}{2\mu}\sin\alpha_{\rm i}\,, \qquad (5)$$

where, μ is the linear absorption coefficient of the material.

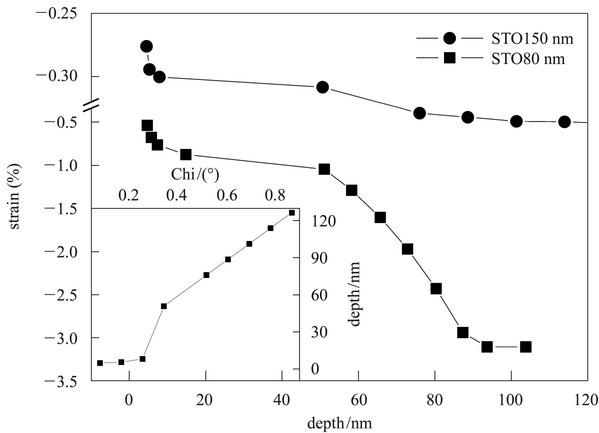

Fig. 4. Depth dependence of in-plane strain for STO(80 nm)/LAO and STO(150 nm)/LAO films.

From the above discussion, we can obtain the structure information from different depths[19]. The depth dependence of in-plane strain for STO(80 nm)/ LAO and STO(150 nm)/LAO in Fig. 4 indicates that the in-plane strain can be divided into three areas: surface layer, strain relaxation layer and interface layer. The thickness of surface layer is about 8 nm, in which the strain changes rapidly. This may be induced by surface tension. If a big lattice mismatch exists, when the film thickness exceeds a certain critical value or the so-called critical thickness, dislocation and other defect will come into being to release the over much accumulative strain energy. Strain relaxation often happens in this process. Generally, the interface layer corresponds to the initial few layers since the film begins to grow. For STO (150 nm)/LAO, the depth of strain relaxation layer is 8—120 nm from surface. This may indicate that the strain is mostly relaxed in the first 30 nm at the beginning of the film growth. This is proved by measuring the in-plane strain of the STO (80 nm)/LAO thin film. The strain is relaxed in a large rate in the first 30 nm, which decreases from −3.1% lattice mismatch at the interface to about −0.81% at the depth of 50 nm from the surface. Because the limitation of penetration depth of X-ray, we didn't get enough structure information for interface layer for the thicker film STO(150 nm)/LAO, while the GIXRD measurement for STO (100 nm)/DSO indicates the critical thickness is almost 30 nm, which is consistent with the value by calculation using Matthews equation[20].

A 2D-RSM shows the map of a region of reciprocal space in the vicinity of each (hkl) reflection. By comparing the profile and position of the reciprocal space mapping from film and substrate, the information such as layer tilt, strain, coherency, relaxation, lattice parameter spread, mosaicity and curvature can be found[21].

When a thin film is deposited on a substrate, the film lattice may be fully strained or at the opposite extreme, fully relaxed. Intermediate, partially relaxed states also occur commonly. For the case of full strain, the matching of the in-plane lattice vector of the film to the substrate necessitates that both the symmetric and asymmetric X-ray reflections of the substrate and film lie vertically above each other in reciprocal space. For a fully relaxed layer, the in-plane vector is free of the substrate constraints. Thus, neglecting such complications as tilt between layer and substrate and curvature, the film and substrate reflections for a fully relaxed layer will lie along a radial line through the origin of the reciprocal space. X-ray reciprocal

space maps on symmetric (002)and asymmetric(103) reflections from the STO(100 nm)/DSO were measured and the typical results are shown in Fig. 5.

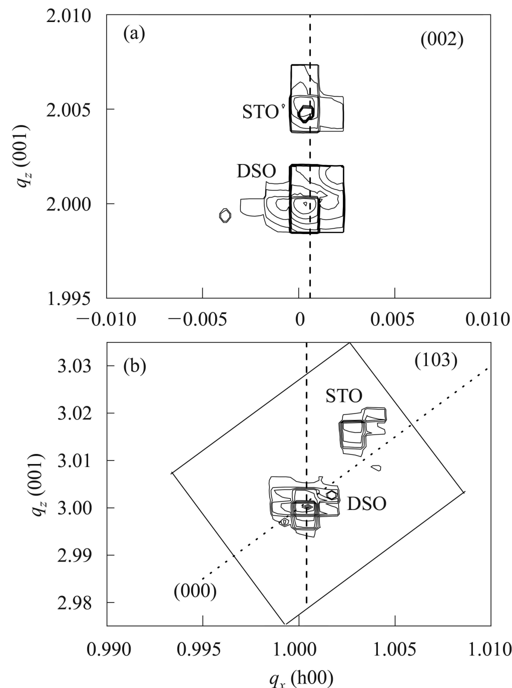

Fig. 5. RSM for the STO/DSO layers. (a) symmetric (002) RSM. The dashed line connects the center of STO and DSO reflection is the assistant line; (b) asymmetric (103) RSM. The dashed line and dotted line correspond to the fully strained and fully relaxed line respectively.

From Fig. 5(a), we can find the assistant line across the center of both the STO film and the DSO substrate is parallel with q_z, which means there is no tilt between the film and the substrate. The STO reflection is tensile alone q_z. Because q_z is inverse proportion to the lattice constants of surface normal, it means relaxation is progressive over depth in the film, which is consistent with our GIXRD experiment. It's obvious that, in Fig. 5(b), the STO reflection locates between the assistant line and the line across the origin of reciprocal space. As discussed above, this indicates the film is partially relaxed, which is also coincident with the GIXRD result.

On the other hand, the STO reflection seems irregular, this may be concerned with the low intensity of (103) reflection and/or defect such as relaxation induced dislocations inside the film.

4 Conclusion

Several kinds of X-ray diffraction technologies and AFM are used to investigate the structure information of STO thin films epitaxially grown on different substrates. We find that the films directly grown on LAO and DSO substrates have a better lattice quality than those grown on the DSO and SRO buffered LAO substrates. GIXRD measurement indicates that the in-plane strain could be divided into three areas for both tensile and compressive strained thin films.

We thank professor Ju Gao, from the University of Hong Kong, Dr. J.H. Hao, from PloyU of Hong Kong, for their sample preparation and useful discussion. Partial GIXRD and RSM datas were collected at the X-ray Diffuse Scattering Station on the 4W1C Beam-line of BSRF.

References

1 Hirota K, Hill J P, Shapiro S M et al. Phys. Rev. B, 1995, **52**: 13195—13205
2 Durán A, Martínez E, Díaz J A et al. J. Appl. Phys., 2005, **97**: 104109—104114
3 Shirokov V B, Torgashev V I, Bakirov A A. Phys. Rev. B, 2006, **73**: 104116—104123
4 Robert Blinc, Bostjan Zalar, Valentin V. Laguta et al. Phys. Rev. Lett., 2005, **94**: 147601—147604
5 Devonshire A F. Theory of Ferroelectrics. Phil. Mag. Suppl., 1954, **3**: 85—130
6 Haeni J H, Irvin P, Chang W et al. Nature, 2004, **430**: 758—761
7 Vasudevarao, Kumar A, TIAN L et al. Phys. Rev. Lett., 2006, **97**: 257602—257605
8 HE Fei-Zhou, Wells B O et al. Phys. Rev. B, 2004, **70**: 235405—235414
9 HE Fei-Zhou, Wells B O, Shapiro S M. Phys. Rev. Lett., 2005, **94**: 176101—176104
10 Pertsev, Zembilgotov N A, Tagantsev A G et al. Phys. Rev. Lett., 1998, **80**: 1988—1991
11 Yamada T, Astafiev K F, Sherman V O et al. Appl. Phys. Lett., 2005, **86**: 142904—142906
12 Sato H, Naito M. Physica C, 1997, **274**: 221—226
13 Bozovic I, Logvenov G, Belca I et al. Phys. Rev. Lett., 2002, **89**: 107001—107004
14 Ayers J E. Journal of Crystal Growth, 1994, **135**: 71—77
15 ZHAI Z Y, LI X Z, ZHI S S et al. Surf. Rev. Lett., 2007, **250**: 182—187
16 Heying B, WU X H, Keller S, LI Y et al. Appl. Phys. Lett., 1996, **68**: 643—645
17 Dosch H. Phys. Rev. B, 1987, **35**: 2137—2143
18 WU X S, CAI H L, XU J et al. J. Appl. Phys., 2004, **95**: 7109—7111
19 ZHAI Z Y, WU X S, JIANG Z S et al. Appl. Phys. Lett., 2006, **86**: 262902—262904
20 ZHAI Z Y, WU X S, CAI H L et al. J. Phys. D: Appl. Phys., 2009, **42**: 105307
21 TAN W S, CAI H L, WU X S et al. Journal of Alloys and Compounds, 2005, **397**: 231—235